

Network-agent based model for simulating the dynamic spatial network structure of complex ecological systems

Taylor M. Anderson*, Suzana Dragičević

Spatial Analysis and Modeling Research Laboratory, Department of Geography, Simon Fraser University, 8888 University Drive, Burnaby, BC, V5A 1S6, Canada

ARTICLE INFO

Keywords:

Network-agent based modeling
Spatial networks
Ecological complex systems
Geographic information systems
Forest insect infestation
Emerald ash borer

ABSTRACT

Non-spatial ecological networks provide insight into the organization and interaction between biological entities. More recently, biological dispersal is modelled using *spatial networks*, static sets of georeferenced habitat patches that connect based on a species' maximum dispersal distance. However, dispersal is complex, where spatial patterns at the landscape scale emerge from interactions between ecological entities and landscape features at much finer individual scales. Agent-based modelling (ABM) is a computational representation of complex systems capable of capturing this complexity. Therefore, this study develops a network-ABM (N-ABM) that combines network and complex systems theory to simulate complex evolving spatial networks. The developed N-ABM approach is implemented on the case study of the emerald ash borer (EAB) bark beetle using geospatial datasets in Ontario, Canada. The N-ABM generates dynamic spatial network structures that emerge from interactions between the EAB and tree agents at the individual scale. The resulting networks are analyzed using graph theory measures. Analysis of the results indicates a relationship between preferential attachment in insect host selection and the emergent scale-free network structure. The N-ABM approach can be used to represent dynamic ecological networks and provides insight into how network structure emerges from EAB dispersal dynamics, useful for forest management.

1. Introduction

Ecologists are largely concerned with the scientific analysis of interactions among species and their environment (Agrawal et al., 2007). To study these interactions, ecological systems are often presented as networks, where the network's nodes represent biological entities and the network's links represent some form of ecological interaction. Sets of ecological interactions are traditionally represented as non-spatial networks and are most commonly grouped into three ecological network types including food webs (Cohen, 1978; Hall and Raffaelli, 1993), host-parasitoid webs (Muller et al., 1999; Morris et al., 2004), and mutualistic webs (Jordano, 1987; Stang et al., 2006). Graph theory, a mathematical characterization of networks, can then be used as a tool to characterize ecological network topology, cross-compare between network structures to find common ground and uniqueness, and understand how network structures affect network dynamics and vice versa (Ings et al., 2009).

Because ecological interactions take place in geographic space and time, it is argued that the framework of ecological networks must also account for these contexts (Fortuna and Bascompte, 2007). Landscape connectivity graphs were one of the first efforts to represent ecological

phenomena as networks in an explicitly geospatial context (Urban and Keitt, 2001). Using orthophotos or classified maps, habitat patches are abstracted as nodes that are embedded in geographic space. The formation of links between nodes signifies the potential dispersal from one habitat patch to another. Since long dispersal distances come at a greater cost (i.e. energy, time), the connectivity between two nodes is typically a function of proximity or adjacency, meaning nodes that are closer to one another have a higher probability of connecting. In these network representations, there are minimal data requirements, needing only the geographic location of habitat patches and maximum dispersal distance of the species of interest (Minor and Urban, 2007). The structure of the landscape connectivity graphs can inform species dispersal patterns, identify keystone patches that are critical to landscape connectivity, and furthermore, assess how dispersal patterns would change in response to disruptions in the network. For example, Fortuna et al., (2006) develop a network of ponds to identify the spatial structure of amphibian dispersal and the species persistence in drought. In another study, Bunn et al. (2000) compare landscape connectivity between two species that share the same habitat and find that the landscape is connected for one and disconnected for the other, presenting implications for conservation biology.

* Corresponding author.

E-mail addresses: taylora@sfu.ca (T.M. Anderson), suzanad@sfu.ca (S. Dragičević).

Table 1

Definitions of important graph theory measures.

Graph Theory Measure	Definition
Node degree k	A local network measure that counts of the number of connections node i has to other nodes
Average node degree $\langle k \rangle$	A global network measure describing the average node degree across all nodes in the network
Degree distribution $P(k)$	A fraction of nodes in the network with degree k
Clustering coefficient C	A local network measure that calculates the likelihood that nodes connected to node i are also connected to each other
Average clustering coefficient $\langle C \rangle$	A global network measures that summarizes the average clustering coefficient across all nodes in the network
Path length l_s	A local network measure calculating the shortest path consisting of a number of nodes or links connecting two pairs of nodes in the network
Average path length $\langle l_s \rangle$	A global network measure calculating the average number of intermediate nodes or links in the shortest path between all pairs of nodes in the network

Despite the potential, network approaches that leverage graph theory for the study of ecological systems in a geospatial context mostly represent ecological systems at the *landscape species-scale* as a fixed network structure on which dispersal takes place (Fortuna et al., 2006). Although useful, spatial ecological networks at this scale are limited in their ability to account for the complexity in emergent dispersal patterns, which often develop from local spatio-temporal dynamics between individuals and their environment. With a few exceptions, spatial ecological networks are rarely scaled down to the *individual species-scale* and as such, it is challenging to make this link between network structure and network dynamics (Dupont et al., 2011). Additionally, data capturing spatio-temporal dynamics at the individual-scale, between large sets of heterogeneous individuals, and across large spatial extents is not typically available for many types of ecological phenomena. Furthermore, field studies to acquire this data is expensive and time-consuming (Minor and Urban, 2007). As such, the development of an experimental setting to better understand the connections between network structure and network dynamics is needed (Stouffer et al., 2010).

Agent-based models (ABM) are computational representations of complex systems that explicitly represent interactions between individual entities or “agents” from which system-level behavior emerges, thus simulating ecological phenomena at a resolution that facilitates the construction of fine-scale networks (Grimm and Railsback, 2013). Developed ABMs are virtual laboratories, permitting exploration of the simulated phenomena and its associated network structure as it responds to local dynamics. ABMs have been developed to represent complex ecological systems over space and time for many ecological phenomena such as fish (Letcher et al., 1996), birds (Travis and Dytham, 1998), caribou (Semeniuk et al., 2012), and forest insect infestation such as the mountain pine beetle (Perez and Dragičević, 2010; Pereira et al., 2011; Bone and Altawee, 2014) and the emerald ash borer (Anderson and Dragičević, 2015, 2016), to name a few. Networks have been integrated with agent-based models (Berryman and Angus, 2010; Kicer and Çırpıcı, 2016); however, these studies typically focus on the topological network structure of systems rather than spatial network structures and thus do not incorporate geospatial datasets.

Therefore, this study proposes the integration of complex systems theory with network theory and geospatial datasets to represent complex spatio-temporal ecological systems using dynamic spatial networks. The main objective of this study is to develop and implement an integrated geospatial modelling approach, a network-ABM (N-ABM), to represent and analyze the dynamic spatial structure of ecological networks. Specifically, the agents’ behavior and interactions form and modify the network over space and time. Graph theory measures are used to measure and characterize the simulated spatial network structures to better understand how network structure evolves over space and time from interactions between biological individuals. The developed N-ABM approach is applied using the case study of a real forest insect infestation, the emerald ash borer (EAB) in Southern Ontario, Canada.

2. Networks and their representations through graph theory

This section provides important network and graph theory definitions from which dynamic spatial network representations and measurement tools are derived. Foundations of graph theory are reviewed comprehensively (Barabási, 2016; Newman, 2003; Lewis, 2011) and for spatial graphs specifically (Barthélemy, 2011). A graph G is a mathematical representation of an observed network reduced to a set of nodes N that are connected by directed or undirected links L . Nodes represent entities that make up the observed network and links represent the interactions between them.

Many empirically-observed networks have properties corresponding to random, small-world, or scale-free graph types. Each graph type is unique in the way that it is formed and its resulting properties. Some common properties are defined in Table 1. The properties defined in Table 1 can be calculated as a local measure for each individual node or averaged across the network as a global measure.

Random graphs are modelled by linking nodes randomly based on probability p (Erdős and Renyi, 1959; 1960). As a result, one property of a random graph is a well-defined average node degree $\langle k \rangle$, producing a Poisson degree distribution $P(k)$. The random connections that form between the set of nodes generate a low average clustering coefficient $\langle C \rangle$, meaning that on average, it is unlikely that nodes connected to node i are also connected to each other. This lack of clustering produces a short average path length $\langle l_s \rangle$ (Boccaletti et al., 2006). Networks observed in the real world rarely exhibit properties of random graphs. However, random graphs provide a baseline for which to compare properties observed in real networks.

Some empirically-observed networks such as social networks have been found to have a much higher average clustering coefficient and a similar average path length than their random counterparts with the same number of nodes and the same average degree. These networks exhibit properties of small-world graphs (Watts and Strogatz, 1998). Small world graphs are modelled as a lattice, where each node is connected to the exact same number of adjacent nodes, and a few nodes are rewired to a randomly chosen node. The establishment of just a few random connections dramatically reduces the average path length between any two nodes in the network, making the movement of material such as information, individuals, and power between nodes highly efficient.

A degree distribution unlike that of a random or small-world graph has been observed in several real networks such as the World Wide Web (Albert et al., 1999), characterized by a small fraction of nodes that have a very large number of links and a large fraction of nodes that have only a few. This degree distribution forms a power law, expressed as:

$$p(k) \sim k^{-\alpha}$$

where the probability p of observing a node with k connections is the number of connections to some negative exponent called a degree exponent α . These observed network structures exhibit the properties of scale-free graphs (Barabási and Albert, 1999). A scale-free graph is

modelled through the process of preferential attachment of new node j to node i based on node i 's degree k . Specifically, new nodes prefer to link to existing nodes that have a higher degree, and thus “the rich get richer”. In addition to a power law degree distribution, empirically-observed networks exhibiting properties of scale-free networks are characterized as having a shorter average path length and a similar average clustering coefficient in comparison to its random network counterpart.

In many cases, real networks can be modelled using a topological or spatial structure. The spatial structure of networks provides valuable information explaining network structure and behaviour. As geospatial data availability increases, geospatial network representations and analysis become more feasible. In a geospatial network, nodes are embedded in geographic space, defined explicitly using geographic coordinates. Geospatial networks are unique from their non-spatial, topological counterparts because any node's degree k is limited by physical space and thus distant connections are costly in terms of energy, money, and time. The structure and dynamics of real spatial networks have been characterized for transportation and infrastructure (Guimera and Amaral, 2004; Jiang, 2007; Watts and Strogatz, 1998) and less commonly for social (Stoneham, 1977; Andris, 2016) and ecological (Fortuna et al., 2006; Pereira et al., 2011) phenomena. Graph theory-based network approaches have been proposed as useful tools in landscape ecology (Ferrari et al., 2007; Minor and Urban, 2007; Urban and Keitt, 2001), however few studies actually operationalize these approaches on real case studies using geospatial data (Andersson and Bodin, 2009; Fortuna et al., 2006; Pascual-Hortal and Saura, 2008; Zetterberg et al., 2010). Furthermore, graph theoretic approaches in landscape ecology are typically limited to static networks at the landscape scale and thus are unable to explore the spatio-temporal complexity inherent to ecological processes. Therefore, this study seeks to develop an integrated modelling approach that can facilitate the exploration of the complex dynamic spatial structure and behavior of real ecological networks such as insect infestation. Specifically, network theory and agent-based modelling (ABM) are integrated to develop an N-ABM.

3. Methods

The developed N-ABM simulates a dynamic spatial network structure that emerges over space and time from interactions between agents at the individual scale (Fig. 1). Graph theory is used to characterize and measure the obtained simulated spatio-temporal network patterns. The proposed approach is implemented and tested on the case study of the emerald ash borer (EAB) bark beetle in the Town of Oakville, Canada (Fig. 2), first discovered in this area in 2008. The N-ABM approach is developed using the Java object-oriented programming language and *Repast Simphony 2.4* (2017), a free and open source Recursive Porous Agent Simulation Toolkit (Repast). Repast Simphony is used for modelling complex adaptive systems through the development of ABMs and has a large and growing community developing a wide range of applications for social, evolutionary, industrial, and ecological

simulations (North et al., 2013).

The following sections first provide an overview of the case study, including the EAB's biological background, followed by a detailed description of the development of the N-ABM and the graph measures used to characterize and analyze the N-ABM simulation outputs.

3.1. Emerald ash borer (EAB) biological background

The emerald ash borer (EAB) *Agrilus planipennis* Fairmaire (Coleoptera: Buprestidae) is an invasive phloem-feeding beetle native to countries in Asia. The EAB was first introduced into North America in the late 1990s (Siebert et al., 2014) and was discovered in 2002 in Detroit, Michigan, US and Windsor, Ontario, Canada (Straw et al., 2013). The EAB is the cause of the decline of the North American ash tree population, creating devastating ecological and economic impacts.

EAB larvae feed on ash tree phloem for one to two years before emerging as adults from under the bark of ash trees to reproduce in early June through August (Cappaert et al., 2005). Mated female EAB locally disperse in search of host trees suitable for offspring. Local dispersal is constrained by the natural flight ability of the EAB, where mated female EAB travel on average 2.8 km in 24 h (Taylor et al., 2007). Dispersal to distances beyond the EABs' natural abilities is referred to as long-distance dispersal. This type of dispersal is facilitated by human transportation of infested wood products and firewood resulting in the establishment of satellite populations beyond the main front of infestation. As a result, ash trees that are near major roads and campgrounds are at high risk (Muirhead et al., 2006).

Mated female EAB use olfactory, tactile, and possibly auditory cues to determine the most suitable hosts for oviposition. It is believed that EAB have specific preferences for ash tree hosts of a certain type, size, location, and level of host tree stress. It has been found that ash tree types with a naturally lower resistance to insect infestations such as the green, black, and white ash, versus their blue ash counterparts, are targeted more frequently (Rebek et al., 2008; Anulewicz et al., 2008). It is also suggested that in order to sustain larval galleries, mated females prefer ash trees that are larger in size (Mercader et al., 2011) and ash trees that are closer in distance to their point of emergence (Mercader et al., 2009).

It is hypothesized that EAB host selection is influenced by volatiles emitted by stressed ash trees. Tree stress is caused by drought, woodpecker damage, wounding, and of course, insect feeding caused by larval galleries such as those produced by EAB. McCullough et al. (2009) and Tluczek et al. (2011) tested this hypothesis by girdling ash trees, a process where a 20 cm wide band of outer bark and phloem is removed, cutting off the flow of water and nutrients within the tree. They found that girdled trees captured significantly more adult EAB and had higher larval densities.

3.2. N-ABM

The purpose of the N-ABM is to represent the dynamic spatial network that emerges from simulated infestation dynamics. Specifically,

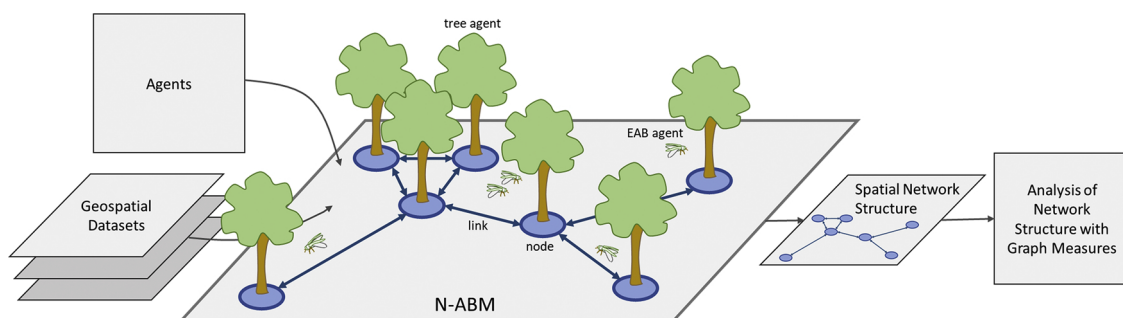


Fig. 1. Network-agent based model (N-ABM) approach applied for emerald ash borer infestation case study.

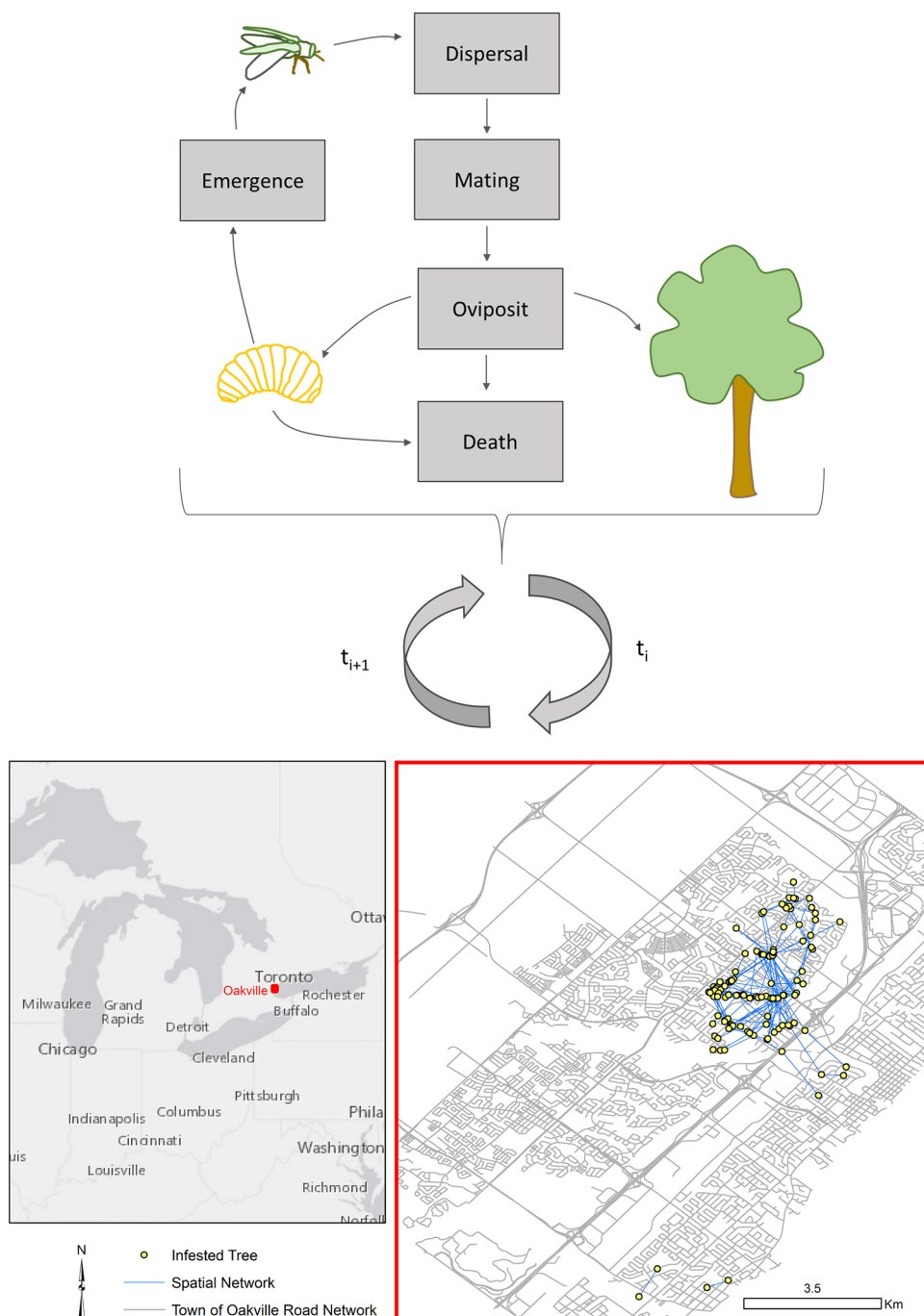


Fig. 2. Overview of the geospatial N-ABM agents' interactions, processes, and scheduling for the simulation of dynamic spatial networks with the map of the study area in Oakville, Canada.

agent interactions between EAB and ash tree agents, implemented by the ABM component of the N-ABM form the basis of the network structure that dynamically evolves over geographic space and time.

The N-ABM is implemented on datasets for the study site, the Town of Oakville, Canada, to represent the EAB infestation from June 1st, 2008 to August 31st, 2009. To account for variation in model outputs as a function of randomness incorporated into ABM processes, the model was run 50 times. The Town of Oakville (study area spanning across 138.5 km²) acquired and developed geospatial data that can in turn used for model creation, calibration, and validation of EAB infestation dynamics. The geospatial data used in this study include the following:

(1) GIS data layers of the tree inventory for the Town of Oakville with

- location and attribute data for all tree species ([Trees, 2018](#));
- (2) GIS data layers containing (a) the location of recreational parks and campgrounds ([Parks Recreation and Culture Guide, 2018](#)) and (b) major streets for the Town of Oakville ([Road Network, 2018](#));
- (3) GIS data layers representing the delimitation of actual EAB infestation according to levels of severity observed in the Town of Oakville in 2009 obtained through Forestry Services, Parks and Open Space, Town of Oakville.

3.2.1. Simulating infestation dynamics using agents

The description of the ABM component of the N-ABM here includes some important elements from the Overview, Design concepts, and Details (ODD) protocol ([Grimm et al., 2006](#)). For a detailed description

Table 2

A description of (A) agent state variables and (B) agent parameters with references.

A. Agent State Variables	Variable	Description	
All agents	Age	Agent age in days	
	Location	Decimal degrees	
Adult EAB	Number of offspring produced	Number of offspring that have been produced by the agent	
	Fertility	Whether the agent is fertile or not	
Larvae	Sex	Sex of the larvae	
Ash Tree	Stress	Stress level associated with larval feeding as a result of infestation	
	Number of larvae	Number of larvae existing within the tree	
B. Agent Parameters	Parameter	Description	Reference
Adult EAB	Maximum flight/day	2.8 km/day	Taylor et al. (2007)
	Chance of successful fertility	82%	Rutledge and Keena (2012)
	Maximum number of offspring	Randomly selected between 60 and 90	Jennings et al. (2014)
	Survival rate of eggs	Randomly selected between 53% and 65%	Jennings et al. (2014)
Larvae	Sex ratio	1:1, 50%	Lyons and Jones (2005)
	Survival rate of larvae	Host tree defense: max 21%, disease: 3%, woodpecker: max 17%	Duan et al. (2010)
Ash Tree	Carrying capacity	44 EAB/ per m ² of bark	Jennings et al. (2014)

of the ABM component that includes all elements, see [Anderson and Dragićević, 2016](#). The purpose of the ABM component of the N-ABM is to simulate interactions between EAB agents and ash tree agents. These interactions are the basis for which the tightly coupled dynamic spatial network forms and evolves over space and time. The ABM component of the N-ABM is based on an existing and validated ABM developed by [Anderson and Dragićević \(2016\)](#) and was previously applied to simulate the biological control of EAB in the Town of Oakville, Canada. The following sections describe how the infestation dynamics are implemented in the N-ABM as a function of agent interactions. [Fig. 2](#) depicts the detailed processes and scheduling pertaining to the interactions between the EAB and the ash tree agents that in turn generate the dynamic spatial networks.

3.2.1.1. Agents and state variables. The N-ABM simulates adult EAB, EAB larvae, and ash tree hosts agents. Using biological information obtained from the literature ([Table 2](#)), agent individuals are programmed with state variables and agent parameters. The state variables ([Table 2A](#)) are associated with the state of the agent at a particular model time step. The agent parameters ([Table 2B](#)) are virtual components that define the agents and shape their behavior.

3.2.1.2. Agent process overview and scheduling. As depicted in [Fig. 2](#), the developed N-ABM simulates EAB behavior for two seasons of infestation from June 1st, 2008 (T_1), when the EAB was first introduced into the Town of Oakville, to the end of August 2009 (T_{457}). Each model time step (T_i) represents one day in the real world. The main processes and schedules of each agent are defined and presented in [Table 3](#). Upon model initialization, the first population of female adult EAB agents emerge from an ash tree and move through their life cycle as a collection of subroutines to simulate real EAB behavior ([Fig. 2](#)). Life cycle stages include emergence, dispersal in search of food, maturing and mating, host selection and oviposition of EAB larvae agents, and once they have oviposited all their offspring, they die. These stages are executed as a function of the agent's age and parameters. The EAB larvae agents grow over time and if they do not die from external factors, a new generation of EAB emerge and begin their life cycles.

Host selection is a process integrated into EAB adult agent decision-making through a host selection algorithm developed by [Anderson and Dragićević \(2016\)](#). The host selection algorithm allows EAB agents to compare between trees within their daily flight radius and optimize their decision of which tree to infest based on their preferences at each time step. Specifically, EAB agents compare ash trees based on the tree's location, type, size, and tree stress. Ash trees are more attractive to the EAB agent in the case that they are the following: 1) a type of ash that

are naturally less resistant to EAB infestation, 2) are closer to the EAB agent's location, 3) are larger, and 4) are of greater stress levels.

On average, 1% of the EAB population is transported by mechanisms of long-distance dispersal ([Taylor et al., 2007](#)). In the model, long-distance dispersal is a random process where each year, 1% of the EAB population has a 30% chance of establishing successfully via long-distance dispersal. The success rate of 30% was determined through model calibration ([Anderson and Dragićević, 2015](#)). Trees that are near major transportation networks or near recreational parks and campgrounds are susceptible to the mechanism of long-distance dispersal. Once a satellite population is established, the adult EAB agent disperses locally and the life cycle continues.

Ash tree agents are represented using tree inventory geospatial data of the Town of Oakville ([Fig. 2](#)), containing the location, type, and size of trees. Each ash tree agent represents an ash tree. Ash tree agents record whether it is infested and the number of larvae feeding on it.

3.2.1.3. Agent initialization. The model is initialized for the time T_1 on June 1st, 2008. Upon initialization, a population of EAB emerge from the North Iroquois Ridge Community (43.47 decimal degrees North and 79.69 decimal degrees West) where the beetle is thought to have first become established in the Town of Oakville ([BioForest Technologies Inc, 2011](#)). Although the initial number of beetle agents to emerge is random, the number falls within a threshold proportional to the carrying capacity of ash trees in the region where a maximum of 44 female adult beetles emerge per m² of the ash trees surface area ([McCullough and Siegert, 2007](#)). The average size of the tree in the initial location of infestation is 13 m², estimated by using the height and DBH recorded in the geospatial tree inventory dataset. As such, the model is initialized in 2008 with a maximum of 572 emerging female EAB agents and, with up to 41% of larval death via host tree defense, woodpecker predation, and environmental factors and disease ([Duan et al., 2010](#)), a minimum of 234 emerging female EAB agents. There are 6153 ash tree agents in the simulation.

3.2.2. Infestation dynamics as networks

In the developed N-ABM approach, agent interactions drive the structure of a dynamic spatial network. The programming logic and pseudocode are presented in [Fig. 3](#), where nodes and links in the generated spatial network correspond to EAB agents and their interactions with the forest environment. This code tightly couples the agent interactions to the generation of spatial networks. If for example, Agent A, represented by node i , interacts with Agent B, a new node j is added as a proxy for Agent B and a link l is created from node i to node j to represent the interaction. In addition, the link l stores the direction of the link (node i is assigned as the Start Node and node j is assigned as the

Table 3

Main processes and schedules of each agent.

Processes	Description	Scheduling
Adult EAB Agents		
Ageing	The age of the agent is stored as a state variable.	At the initialization of an agent, agent age is equal to 0 days. With each model time step representing one day, age is increased by 1.
Emergence	EAB larvae agents emerge as adult EAB agents.	When EAB larvae agents reach the age of 340 days and if the larvae is female, they emerge as adults EAB agents.
Dispersal	Dispersal is the process whereby agents change location. Dispersal is a function of the host selection algorithm where a distance of 2.8 km/day bounds the EAB's information regarding host tree availability.	EAB agents locally disperse immediately after emergence.
Mating	EAB agent fertility is a function of the chance of fertility parameter. Mated females who are fertile are randomly assigned a maximum number of offspring.	EAB agents mate 7 days after emergence.
Oviposition	Mated fertile EAB are able to compare trees that fall within their daily flight distance radius. The comparison between trees by EAB agents is controlled by the host selection algorithm. Once selected, EAB will oviposit a random number of offspring within its maximum number of offspring onto the selected host.	If fertile, adult EAB begin oviposition 10 days after emergence.
Death	Adult EAB agents die once they have produced their maximum number of offspring.	Triggered when parameter maximum number of offspring is equal to offspring produced.
EAB Larvae Agents		
Ageing	The age of the agent is stored as a state variable.	At the initialization of an agent, agent age is equal to 0 days. With each model time step representing one day, age is increased by 1.
Death	Larvae agents die via external factors.	External factors are applied once in the lifetime of the EAB larvae.
Tree Agents		
Ageing	The age of the agent is stored as a state variable.	At the initialization of an agent, agent age is equal to 0 days. With each model time step representing one day, age is increased by 1.
Become Infested	Ash trees become infested once an adult EAB has chosen it as a host and successfully oviposited their eggs in the tree. The number of larvae feeding on the tree proportionally increases the stress of the tree agent.	Triggered when number of larvae is greater than 1.

End Node).

Using the case study of the EAB infestation as an example, the N-ABM generates a series of graphs G , composed of a growing set of nodes N that in this case represent infested trees at x, y location. Directed links L represent the movement of a mated female EAB agent and form as it moves from infested tree node i to a new tree node j , infesting tree node j . Connections are made to both trees that are not already infested and to trees that are infested and thus are already included in the infestation network.

3.3. N-ABM testing

The spatial networks form as a direct result of the interactions between EAB and ash tree agents over geographic space and time and as such, testing the validity of the ABM component of the N-ABM is important. The N-ABM uses the same agent reasoning and programming code from the validated ABM developed by [Anderson and Dragićević \(2016\)](#). To account for variation in model outputs as a function of randomness incorporated into ABM processes, the model is run 50 times. The simulated state of each tree was determined as a function of the state of each ash tree (infested vs. not infested) in the majority of model runs. The model was validated using a binary confusion matrix that measures the agreement between the simulated state of each ash tree and the state of the corresponding ash tree as observed in the real-world for the same time-period with an overall accuracy of 72%. Additionally, a confusion matrix was used to measure the agreement between the simulated level of severity of each ash tree (low, medium, high) and the level of severity observed in the real world for the corresponding tree with an overall accuracy of 64%. The sensitivity of the model outputs to changes in parameters, most notably to changes in EAB preferences in the host-selection process, were tested using sensitivity analysis ([Anderson and Dragicevic, 2018](#)).

3.4. Analysis of generated spatial networks

Graph theory ([Newman, 2003](#)) provides the theoretical and mathematical foundation for the representation and analysis of network

structures. A primary objective in network analysis using graph theory is to determine the type of network, specifically whether the observed network structure exhibits random, scale-free, or small-world properties. This can be determined using a few global network measures that characterize the network at the network-level: average node degree $\langle k \rangle$, degree distribution $P(k)$, average clustering coefficient $\langle C \rangle$, and average path length $\langle l_s \rangle$. As such, to determine network type, the above measures are calculated for the networks generated by the N-ABM and the obtained values are compared to the expected values if a network with the same number of nodes was random. Therefore, an equivalent random network model N-ABM_{RAND} is developed where EAB agent host selection is programmed as a random process. The average node degree $\langle k \rangle$, degree distribution $P(k)$, average clustering coefficient $\langle C \rangle$, and average path length $\langle l_s \rangle$ is calculated for the N-ABM and the N-ABM_{RAND} and compared.

A detailed description of the selected graph theory measures programmed for the spatial analysis of the generated network structures are as follows:

3.4.1. Average node degree

The number of nodes j that node i is connected to is referred to as the node degree k of i . In an undirected network, the average node degree $\langle k \rangle$ is defined as:

$$\langle k \rangle = \frac{2L}{N}$$

where L represents the number of links in the network and N represents the number of nodes in the network. However, not all graphs are undirected. Movement, for example, a common dynamic modelled in spatial ABMs, is directional, where EAB agents move from a location to a location. Thus, it is important to differentiate between the ingoing links k_{in} with outgoing links k_{out} . Node total degree k in a directed network is defined as:

$$k = k_{in} + k_{out}$$

The average node degree $\langle k \rangle$ in a directed network is defined as:

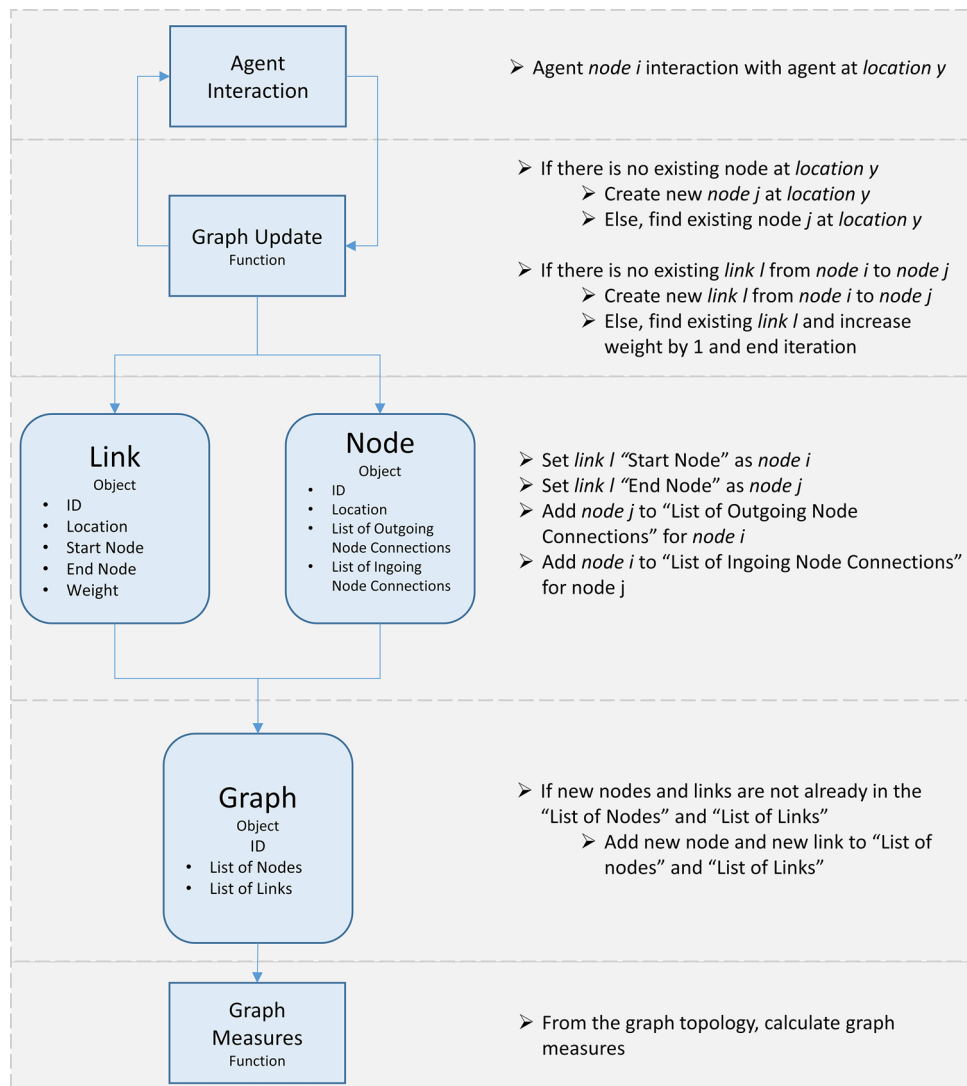


Fig. 3. Programming logic and pseudocode developed for the N-ABM approach that couple agent interactions and the generation of the dynamic spatial network structures.

$$\langle k \rangle = \frac{L}{N}$$

3.4.2. Degree distribution

The degree distribution $P(k)$ calculates the fraction of nodes in a network with degree k , k_{in} , or k_{out} . Using the example of degree k , the fraction of nodes in a network with degree k can be calculated by the number of the nodes with the same degree, divided by the total number of nodes in the network N . For example, if there are four nodes in the network where $k = 1$, and there are a total of 10 nodes, $P(k) = 0.4$. $P(k)$ can be plotted on a histogram to present the degree distribution of the network. The degree distribution is tested for goodness of fit using *powerlaw*, a Python package for analysis of heavy-tailed distributions (Alstott et al., 2014)

3.4.3. Average path length

A path P_{i_0, i_n} that connects the nodes i_0 and i_n in a graph $G = (N, L)$ is defined as an ordered collection of $n + 1$ nodes $N_P = \{i_0, i_1, i_2, \dots, i_n\}$ and *nedges* $L_P = \{(i_0, i_1), (i_1, i_2), \dots, (i_{n-1}, i_n)\}$. The shortest path length between any two nodes in the network model l_s is calculated by implementing Dijkstra's shortest path algorithm into the N-ABM (Dijkstra, 1959), an algorithm developed to find the shortest number of links connecting any two pairs of nodes in the network. Average path

length $\langle l_s \rangle$ is defined as the average value of l_{ij} .

3.4.4. Average clustering coefficient

The clustering coefficient C measures the probability that nodes j connected to node i are also connected to each other (Watts and Strogatz, 1998). When $C = 1$, all nodes connected to node i are connected to each other. When $C = 0$, nodes connected to node i are not connected to each other, generating a star-like structure. The clustering coefficient is formulated as:

$$C(i) = \frac{E_i * 2}{k_i(k_i - 1)}$$

where for node i of degree k_i , E_i is the number of edges among the neighbours of i . The average clustering coefficient is formulated as:

$$\langle C \rangle \sim \frac{1}{N}$$

where the brackets denote the average clustering coefficient over the network.

4. Results

This section presents the N-ABM simulation outcomes and the

Table 4

Summary of network measure results derived from (A) the single N-ABM infestation network chosen for visual presentation of results, and (B) the average value across all 50 generated infestation networks for all network measures with the associated standard error.

	A. Single Network	B. 50 Networks	
	Value	Average Value	Standard Error
Degree and Degree Distribution (k_{out})			
$\langle k_{out} \rangle$	neighboring nodes	4.48 neighboring nodes	0.0146
k_{max}	64 neighboring nodes	61.22 neighboring nodes	0.4755
k_{min}	1 neighboring node	1 neighboring node	0
Degree distribution	Power law	Power law	
$p(k) \sim k^{-\alpha}$	$\alpha = 1.58$	$\alpha = 1.59$	0.0019
Degree and Degree Distribution (k_{in})			
$\langle k_{in} \rangle$	4.48 neighboring nodes	4.33 neighboring nodes	0.0191
k_{max}	52 neighboring nodes	56.46 neighboring nodes	0.5140
k_{min}	1 neighboring node	1 neighboring node	0
Degree distribution	Power law	Power law	
$p(k) \sim k^{-\alpha}$	$\alpha = 1.59$	$\alpha = 1.59$	0.0020
Clustering Coefficient			
$\langle C \rangle$	0.030	0.034	0.0002
Path Length			
$\langle l_s \rangle$	11.27 nodes	11.26	0.0021

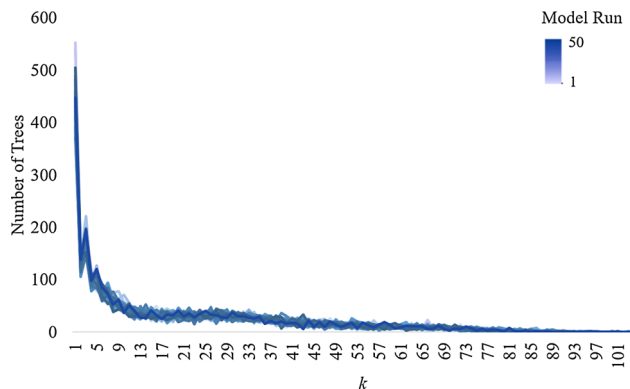


Fig. 4. Variation of the degree distribution $P(k)$ generated across all 50 model runs. The degree distribution presents the number of trees with degree k .

analysis of the generated spatial network structures. To account for stochasticity in generated network structures, the N-ABM is executed 50 times, thus generating 50 different simulation outcomes. The average values and the standard error across all 50 model runs for average node degree $\langle k \rangle$, degree distribution $P(k)$, average clustering coefficient $\langle C \rangle$, and average path length $\langle l_s \rangle$ are calculated and presented in Table 4. The obtained standard error for each network measure is very small, indicating that the N-ABM generates very similar network structures across all runs. This is supported by visibly similar power law degree distributions $P(k)$ across all 50 simulated network structures as presented in Fig. 4 accompanied by minor differences in the calculated alpha exponent (Table 4). Large amounts of variation across several ABM outputs typically points to stochastic uncertainty (Brown et al., 2005), however the minor variation observed in network structure across 50 model runs suggests that the emergent network structure is a function of the generative mechanisms that are implemented in the model, rather than randomness. Therefore, using one network as example to present the results is a viable option as other 49

networks have similar network structure, indicated by the similar obtained network measures for each. Based on this analysis and for the purpose of clarity and visual presentation of the generated maps with network structures, one example network is selected and presented in the following sections.

4.1. Simulation results

Fig. 5 presents one full model run of the N-ABM representing the spread of EAB infestation across the Town of Oakville, Ontario from 2008 to 2009. Specifically, Fig. 5 shows both the infestation extent as a function of the EAB and tree agents' interactions and the generated spatial network structures for time T_i . Particularly, simulation outputs for July 2008 at T_{61} (Fig. 5 A1 & A2), August 2008 at T_{92} (Fig. 5 B1 & B2), July 2009 at T_{426} (Fig. 5 C1 & C2), August 2009 at T_{457} (Fig. 5 D1 & D2) are presented. The EAB are most active during the month of July and August, and therefore, the most notable changes in network structure are visible. The infestation extent as a function of the agent interactions (Fig. 5 A1, B1, C1, and D1) and the network structures (Fig. 5 A2, B2, C2, and D2) are extracted as separate geospatial layers for better visualization; however, both are derived from the same model run. Following model initialization in 2008, EAB spreads locally outward from the epicenter in the north-eastern half of the city. From the epicenter, clusters of infestation develop to the south-east and the west of the epicenter. A satellite population develops in the southern end of the city and in 2009, the second year of EAB infestation, the satellite population, and the main infestation front merge. This is referred to as a stratified dispersal pattern, commonly observed in real-world EAB spread (Muirhead et al., 2006).

4.2. Analysis of the spatial network structure results

Using the topology of the example simulated EAB infestation network in August 2009 derived from the N-ABM at the final time step T_{457} , the resulting graph theory measures are summarized in Table 4.

4.2.1. Graph size

The EAB infestation network in August 2009 is composed of 2540 nodes, meaning that there are just over 2500 infested trees in the network. The number of links or dispersal pathways connecting these nodes or infested trees is 27,560.

4.2.2. Average node degree and degree distribution

The k_{out} and k_{in} measures mathematically characterize different dynamics in the infestation network. A $\langle k_{out} \rangle$ value of 4.48 indicates that on average, EAB agents move from infested tree node i to 4.48 other tree nodes j . Therefore, k_{out} characterizes the local connectivity of each tree node i to other desirable trees j in its proximity. A $\langle k_{in} \rangle$ value of 4.40 indicates that on average, EAB agents move from 4.40 other tree nodes j to tree node i . Therefore, k_{in} characterize the desirability of tree node i .

The max degree k_{max} for k_{out} is 64 and the min degree k_{min} for k_{out} is 1. The max degree k_{max} for k_{in} is 52 and the min degree k_{min} for k_{in} is 1. The values of degree do not indicate the volume of beetles that move across these links, but rather, that several beetles move along each path from node i to node j . The volume of beetles can be represented by node or link weights; however, node and link weights are not included in this network representation to maintain simplicity. The degree distribution $P(k_{out})$ and $P(k_{in})$ can provide information regarding the type of network that emerges from dynamics at the local scale. The $P(k_{out})$ and $P(k_{in})$ are plotted as histograms in Fig. 6A and 6B respectively and as a log-log plot in Fig. 6C and D. The histograms in Fig. 6A and 6B indicate that there are a large fraction of nodes in the network with a very small degree and a small fraction of nodes in the network with a very large degree. In the log-log plot (Fig. 6C and D), this distribution can be described as linear distributions with heavy tails.

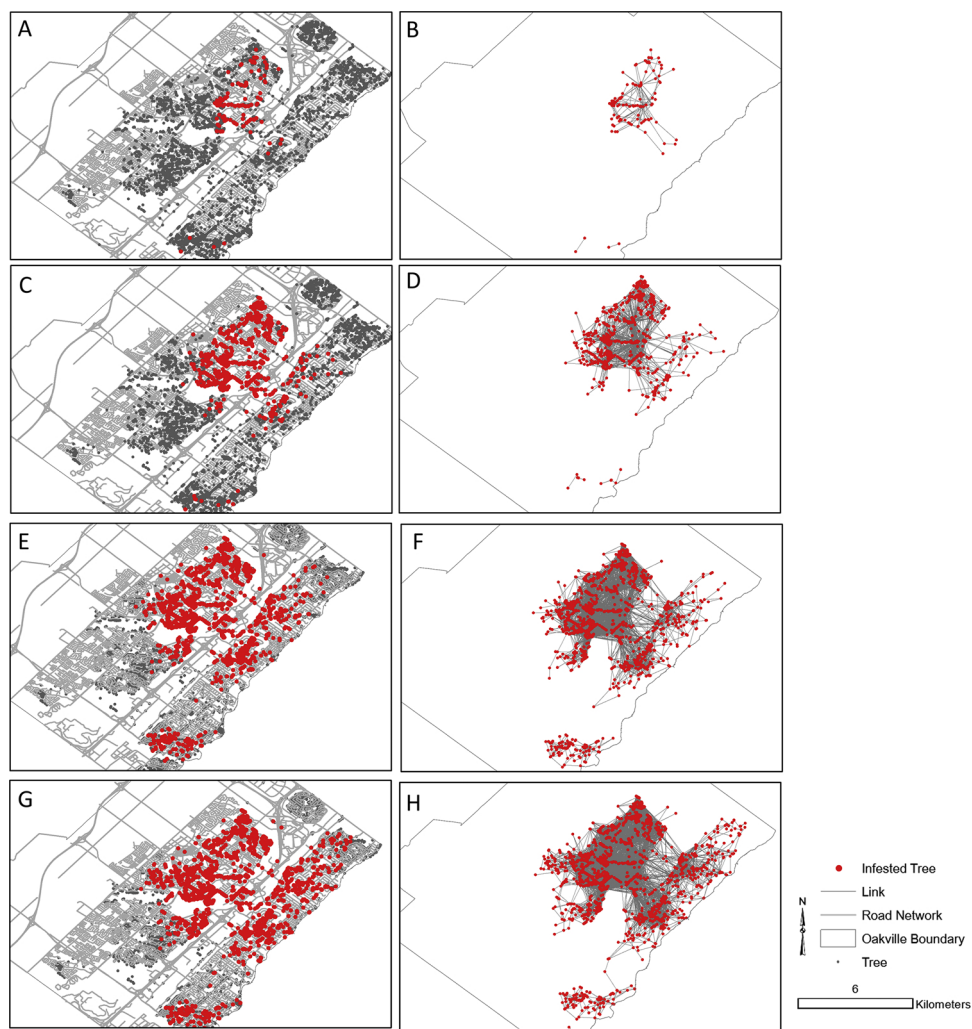


Fig. 5. The N-ABM simulation results depicting spatial EAB infestation extent as a function of EAB and ash tree agents' interactions in the Town of Oakville between 2008 and 2009 for: (A1&A2) July 2008 at T_{61} ; (B1&B2) August 2008 at T_{92} ; (C1&C2), July 2009 at T_{426} ; and (D1&D2) August 2009 at T_{457} .

The degree distribution for $P(k_{out})$ and $P(k_{in})$ can be described as a power law distribution. The distributions produce an alpha exponent $-\alpha$ of 1.58 and 1.59 for $P(k_{out})$ and $P(k_{in})$ respectively and a standard error sigma σ of 0.01 for both. The Kolmogorov-Smirnov distance D is also small with a value of 0.16 for both. The goodness of fit of the degree distribution between a power law and an exponential distribution is first compared, producing a log likelihood ratio R between the two candidate distributions that indicates a power law is a better fit than an exponential with a p-value of 0.0072 and 0.04 for $P(k_{out})$ and $P(k_{in})$ respectively. The directed degrees are also presented spatially (Fig. 7A and B). For both k_{out} and k_{in} , there is a distinguishable core region composed of ash trees that have a high node degree k , surrounded by a large perimeter composed of ash trees that have a low node degree k .

Node degree k appears to coincide with real-world EAB infestation severity (Fig. 7C; Table 5). This is determined by classifying all tree nodes into *high*, *medium*, *low*, and *zero degree* classes based on their simulated degree. The degree of a tree is classified as *high degree* if it falls > 1.5 standard deviation, *medium degree* if from 0.5 to 1.5 of the standard deviation, and as *low degree* if it falls < 0.5 of the standard deviation. All trees with a simulated node degree of zero are classified as *zero degree*. Using a confusion matrix approach (Congalton, 1991), the simulated degree class of each tree node is compared to *high*, *medium*, *low infestation* severity in addition to *no infestation* observed in the real world for 2009 for the same tree. The overall spatial similarity

is 67% where trees with a simulated high degree and medium degree corresponds moderately well with high (18% omission and 36% commission) and with medium (33% omission and 18% commission) infestation severity in the real world respectively. This is not a model validation metric because since the network is not weighted, the tree node degree does not necessarily correlate with tree population density and thus cannot be compared to infestation severity. However, it does indicate that trees that have a high degree in the infestation network are thus are highly spatially accessible and may influence infestation severity.

4.2.3. Degree distribution across time

Using the developed N-ABM approach, all graph theory measures can be calculated at any point in time to better understand the change in network structure as it grows and evolves. The degree distribution $P(k_{out})$ is used here as an example. In each model time step the $P(k_{out})$ of the infestation network maintains a power law. The power law in the early stages of the infestation has an exponent of 3.34. Over time, the exponent decreases before settling at 1.58 (Table 6). The generated power laws indicate that at the beginning of each season of EAB infestation there is a burst of new EAB dispersal where the network is expanded over geographic space and infested tree nodes with a low degree are added to the network. The season of EAB infestation continues and links form between trees that already exist in the infestation network as EAB dynamics such as attraction to trees of ash species,

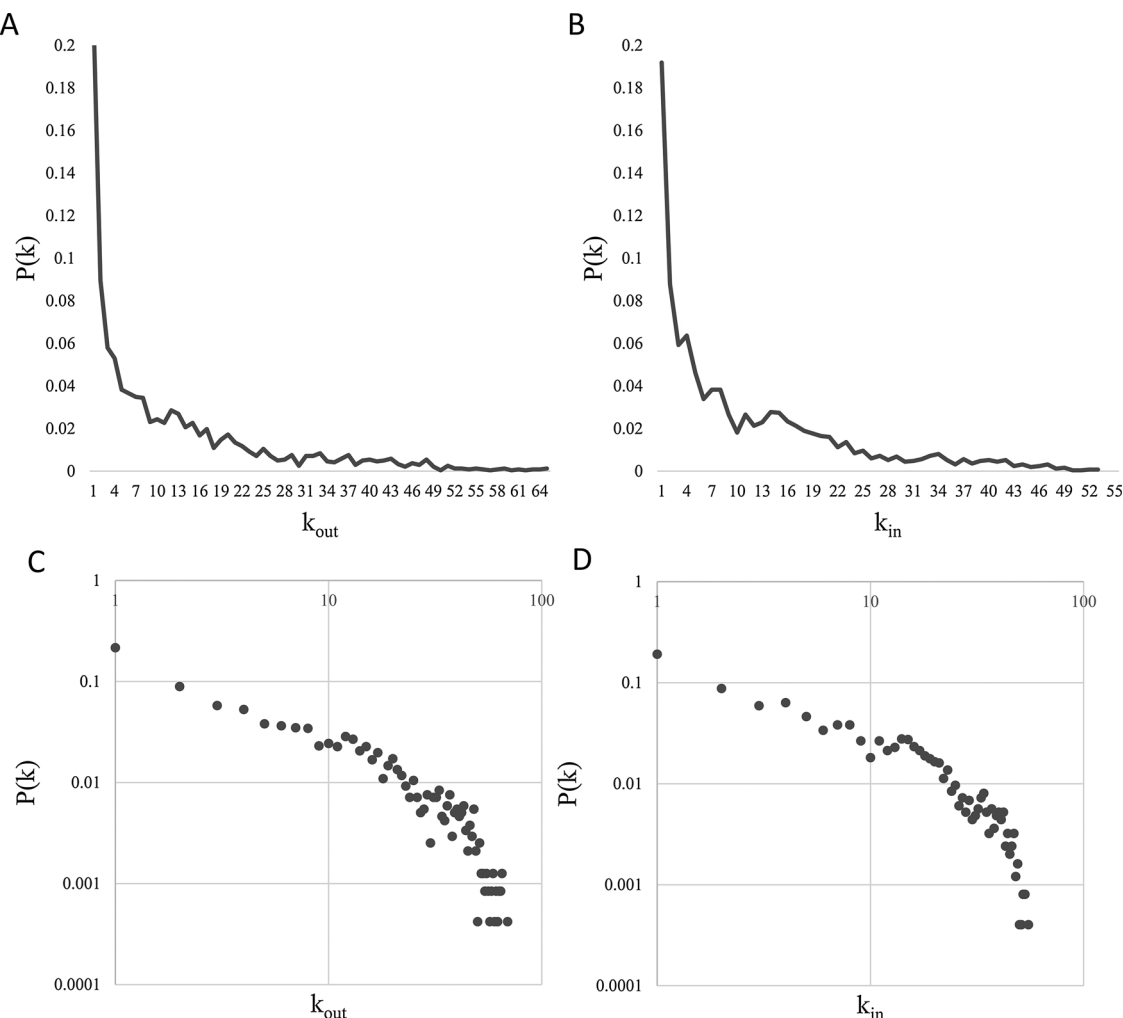


Fig. 6. Degree distribution $P(k)$ for (A) k_{out} and (B) k_{in} and degree distribution $P(k)$ plotted on a log-log scale for (C) k_{out} and (D) k_{in} .

attraction to stressed trees, and carrying capacity begin to play a role in the network structure. This process is quantified by the changes in the power law degree distributions over time, where the power law in early months of infestation has a much higher fraction of tree nodes with a low degree than in the following months.

4.2.4. Average clustering coefficient

The average clustering coefficient is 0.03 meaning that node linkages form a "star-like" pattern. Most of the core region of infested trees is composed of trees with a very low clustering coefficient, meaning that only a few of the nodes that are connected to node i are also connected to each other. In total, there are only three trees with a clustering coefficient of 1, where all nodes that are connected to node i are also connected to each other. We can present this spatially to highlight where clusters exist (Fig. 8). The majority of the nodes with high clustering are near the perimeter. This is potentially an edge effect, where EAB agents can 'no longer' spread due to artificial administrative town boundary and thus continue to infest trees in close proximity resulting in a higher clustering coefficient near the town administrative boundary.

4.2.5. Average path length

The average path length is short, with an average of 11 intermediate nodes that make up the path between any two nodes in the network. This indicates that as a function of the spatial distribution of ash tree hosts and the flight dynamics of EAB, EAB are capable to spread across long distances in a short period of time.

Using the topology of the simulated EAB infestation network in August 2009 derived from the N-ABM_{RAND} at the final time step T_{457} , the resulting graph theory measures are summarized in Table 7.

Comparing the obtained N-ABM analysis results for the case study of the EAB with the N-ABM_{RAND} indicates that the N-ABM spatial infestation network structure is scale-free with hub and spoke architecture, formed by a power law degree distribution for both $P(k_{out})$ and $P(k_{in})$ with an exponent α of 1.58 and 1.59, respectively. Specifically, the short average path length of the N-ABM at 11.27 nodes in comparison to the average path length of the N-ABM_{RAND} at 22.86 nodes. In addition to a power law degree distribution, an average path length in a network that is less than the average path length of its equivalent random network is a defining feature of a scale-free network (Barabási, 2016).

Characterization of emergent spatial network structure can provide insight into network dynamics. For example, if instead of a scale-free network, a random network structure was formed, this would indicate that the underlying processes driving the emergence of the spatial network structure are random. At the most basic level, scale-free networks form as the result of two simple generative mechanisms: growth and preferential attachment, also known as the "rich get richer" phenomenon. In preferential attachment, the probability that a new node becomes connected to an existing node is a function of the existing node's degree. The higher the degree, the more likely the node will form a connection.

To understand why the scale-free network structure emerges, the generative mechanisms included in the N-ABM can be examined. A

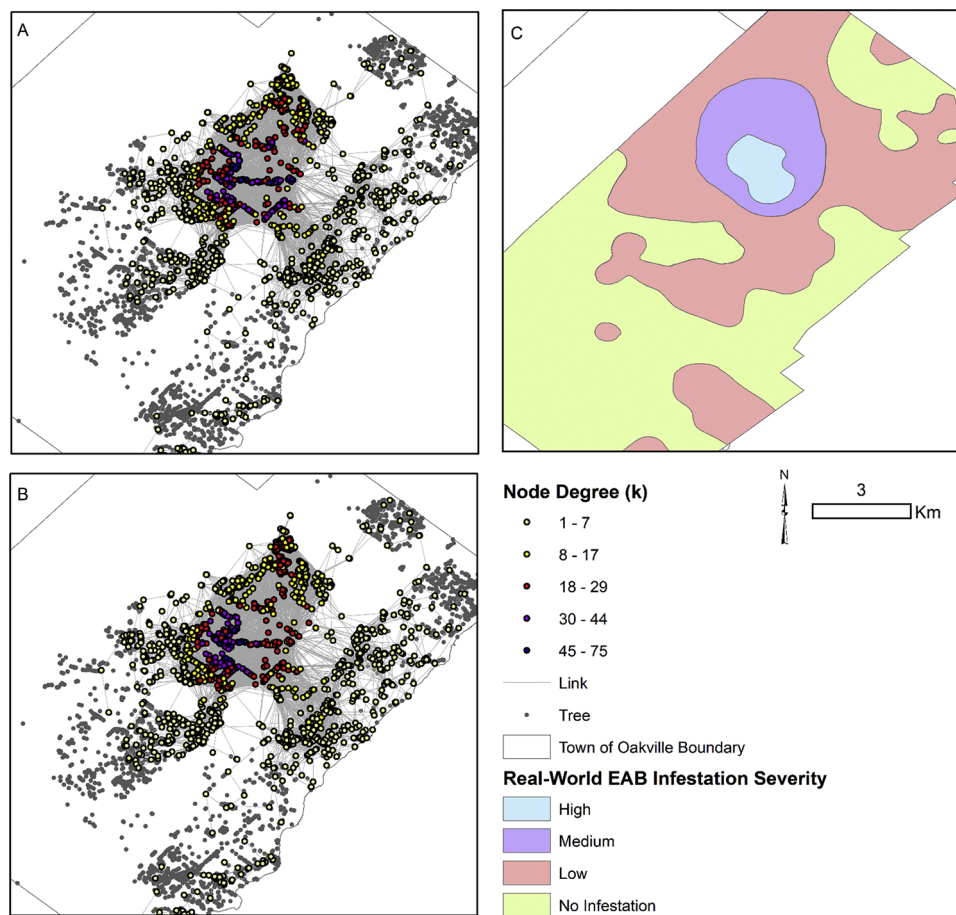


Fig. 7. Spatial distribution of tree node degree for (A) k_{out} and (B) k_{in} demonstrating highly connected trees and less connected trees for EAB insect infestation. The simulated high degree trees correspond to the (C) regions of real-world high severity infestation.

correlation between degree and tree stress at $r^2 = 0.87$ indicates that the EAB host selection process, specifically the EAB attraction to stressed trees, is responsible for the generation of dynamics of preferential attachment and thus the emergent scale-free network structure. In the real world, trees that are preferable for oviposition are infested, resulting in the release of stress volatiles. This creates a positive feedback where as ash trees suitable for host selection become increasingly infested, stress volatiles are released, and thus the trees are increasingly targeted for attack. Networks generated by preferential attachment tend to have high degree nodes or hubs near the center of the network with node degrees that gradually declines toward the perimeter and outer edges of the network. This emerging pattern is produced in the developed N-ABM.

Further analysis of the network structure does not indicate a significant relationship between node degree and tree size or node degree and tree type. Non-spatial scale-free models are not constrained by

Table 6
Power law exponent $-\alpha$ over time.

Date	Model Time Step	Exponent $-\alpha$
June 2008	T_{30}	3.3
July 2008	T_{61}	2.7
August 2008	T_{92}	2.7
June 2009	T_{395}	2.1
July 2009	T_{426}	1.6
August 2009	T_{457}	1.6

space, and thus commonly contain long-distance linkages to non-adjacent nodes, however, in the spatial N-ABM, long-distance links come at a cost and thus are limited to the natural dispersal distance of the EAB (Taylor et al., 2007). The lack of relationship between node degree and tree size or tree type may be a result of the heterogeneous nature of

Table 5

Confusion matrix detailing the spatial agreement of the levels of severity of infestation observed in the real world and simulated node degree.

		Real world tree infestation severity				Commission
		Not Infested	Low Infested	Medium Infested	Highly Infested	
Simulated Tree Degree	Zero Degree	2435	1556	10	0	39.15%
	Low Degree	95	1209	186	0	18.86%
	Medium Degree	0	88	478	17	18.02%
	High Degree	0	0	42	73	36.53%
Omission		3.76%	57.63%	33.25%	18.89%	67.77%

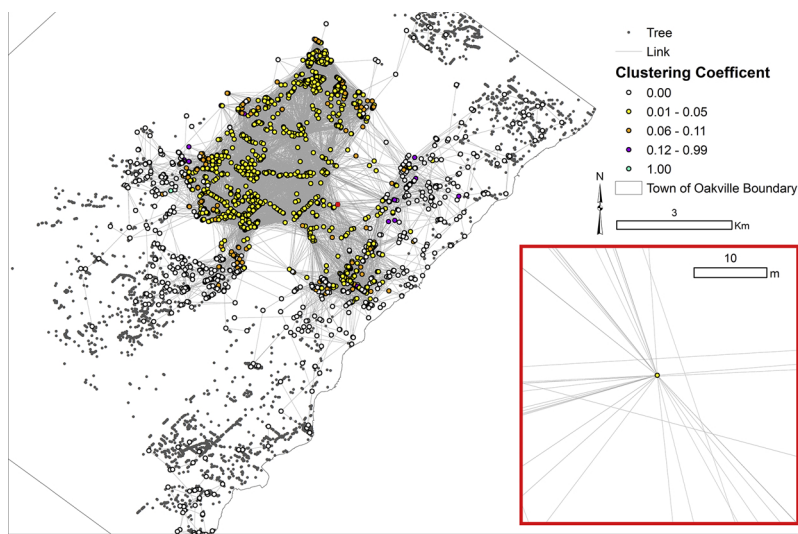


Fig. 8. Spatial distribution of varying clustering coefficients of tree nodes. The inset map corresponds with the red dot on the main map and presents a node exhibiting the star like pattern commonly generated during the EAB host selection process (For interpretation of the references to colour in this figure legend, the reader is referred to the web version of this article.).

Table 7

Summary of network measure results derived from the N-ABM_{RAND} infestation network.

Graph Size	$\langle N \rangle$	2540 nodes
	$\langle L \rangle$	3788 links
Degree and Degree Distribution (k_{out})		
$\langle k_{out} \rangle$	6.4 neighboring nodes	
k_{max}	38 neighboring nodes	
k_{min}	1 neighboring node	
<i>Degree distribution</i>	Poisson	
Degree and Degree Distribution (k_{in})		
$\langle k_{in} \rangle$	6.4 neighboring nodes	
k_{max}	17 neighboring nodes	
k_{min}	1 neighboring node	
<i>Degree distribution</i>	Poisson	
Clustering Coefficient	$\langle C \rangle$	0.007
Path Length	$\langle l_s \rangle$	22.86 nodes

host trees in the environment and the limitation of generating long-distance links. Trees of the most attractive type in the study area may not be available within the flight distance radius allotted to the EAB agent per day, leaving agents to choose the largest or best type available to them at a closer proximity.

Based on the obtained simulation, results suggest that the emergent spatial pattern of EAB spread are primarily a function of the generative mechanisms of preferential attachment based on tree stress, tree distance, and growth or continuing spread of infestation over time. In this study, it is empirically demonstrated that in the same way scale-free networks emerge from growth and preferential attachment, patterns of EAB insect infestation emerge from host selection dynamics over time. Furthermore, the characterization of network structure can provide additional insights useful for pest management. For example, scale-free networks are particularly robust to the removal of nodes at random, meaning that an impactful removal of trees would need to be highly strategized.

5. Discussion and conclusion

Exploring the influence of the spatial structure of the landscape on ecological processes is critical. Landscape connectivity graphs are more recently implemented for this purpose, but are typically static network

representations at a single scale. As a result, landscape connectivity graphs are unable to capture the complexity in dispersal processes whereby interactions at the local scale generate spatio-temporal dispersal patterns at the larger scale. For example, in the case of insect infestation, it is important to explore how interactions between EAB and varying spatial distributions of ash tree hosts generate large-scale spatio-temporal patterns of infestation.

The inclusion of complexity in spatial ecological network approaches can characterize and quantify spatio-temporal patterns in ecological systems that might otherwise be described in a more qualitative manner, identify the underlying interactions and generative mechanisms that drive the emergence of these spatio-temporal patterns, and quantitatively link dynamics at local scales to emergent patterns at larger scales. Therefore, this study proposes the integration of the complex systems modelling approach ABM with spatial networks for the development of a network-based ABM. The approach is demonstrated in application to the case study of the forest insect infestation, EAB. The N-ABM approach facilitates the exploration between network dynamics and network structure, and in this case, links the EAB attraction to stressed trees at the individual scale to dispersal patterns at larger scales. This effectively supports findings in the literature that point to tree stress as the primary factor in host selection (McCullough et al., 2009; Tluczek et al., 2011). The approach facilitates the shift from the characterization of network structure to explaining and identifying the underlying interactions that drive the emergence of a dynamic and evolving spatial network structure.

Across all 50 model runs, stochastic processes within the N-ABM produce a distribution of unique spatial networks, however results show that each of the simulated spatial networks have a highly similar structure. This conclusion is supported by the fact that all spatial network measures for all 50 networks deviate only slightly from the mean and thus have a small standard error. As such, any selected model run would be fairly, although not perfectly, representative of the complete distribution of networks. Therefore, only one randomly selected network from one model run is presented in detail. This serves the purpose of clarity, since it would be overwhelming to visually present all 50 network structures. In future work, it may be useful to develop an approach to summarize a distribution of spatial networks that emerge from the same local processes. Averaging the degree of each node across all 50 model runs is insufficient because it would result in a smoothing effect that would ultimately negate network degree heterogeneity, which is of great interest in network studies. In summary, as a function of the randomness of the N-ABM, the spatial pattern of EAB spread varies from model run to model run, but the network structure does not, presenting a clear link between network dynamics and

network structure. Detailed analysis of the variation of the spatial patterns of EAB spread across model runs resulting from the ABM component used in the N-ABM can be found in [Anderson and Dragićević, 2016](#) [2018](#).

Spatial ecological networks can be represented and analyzed at a variety of scales. Nodes can represent ecological entities from the individual level to various aggregations of individuals (community level, population level, landscape level). The modifiable aerial unit problem (MAUP) is a phenomenon where statistical outputs vary as a function of the level of aggregation in the model. This suggests that the emergent network structure may be a function of the scale at which the phenomenon is represented. However, the aim of the study is to integrate complexity into spatial ecological networks using an agent-based modelling approach, justifying the use of individual-scale representation. It would be desirable to validate the spatial networks themselves generated by the N-ABM. Unfortunately, the nature of the ecological data and current data collection tools and methods cannot provide network datasets and therefore a model of this kind cannot be validated in this context. However, the validation of the ABM agent processes and interactions integrated in the N-ABM that generate the spatial networks gives confidence that the spatial networks are being represented correctly.

In conclusion, the novel N-ABM modelling approach presented here is unique and particularly relevant for modelling complex ecological systems, as there is a demand for the exploration of dynamic ecological networks in a spatial and temporal context. The application of graph theory to the networks generated by the N-ABM helps to better understand, measure, and analyze the influence of geographic space and network structure on network dynamics as well as characterize dispersal patterns, particularly useful from an ecological management perspective. The N-ABM framework is also highly general and flexible as to facilitate the representation and simulation of many ecological systems as dynamic evolving networks. Graph theory provides a large toolset of additional measures that can also be applied for further understanding interactions between other ecological species and the landscape, useful for ecological management or conservation. For example, graph theory measures such as betweenness centrality and link weights can help important habitat features and dispersal pathways that are essential to the connectivity of the landscape for an endangered species and thus be targeted for protection by ecological conservationists and decision makers.

Acknowledgements

This study was fully funded by a Natural Sciences and Engineering Research Council (NSERC)Canadian Graduate Scholarship-Doctoral (CGS D) and the Discovery Grant awarded to the first and second author respectively. The Town of Oakville, Canada provided the datasets. We thank Compute Canada WestGrid high-performance computing facility for enabling agent-based model simulations. The authors are thankful to the anonymous reviewers and the journal Editor for the valuable and constructive feedback on the previous versions of this paper.

References

- Agrawal, A.A., Ackerly, D.D., Adler, F., Arnold, A.E., Cáceres, C., Doak, D.F., Post, E., Hudson, P.J., Maron, J., Mooney, K.A., Power, M., Schemske, D., Stachowicz, J., Strauss, S., Turner, M.G., Werner, E., 2007. Filling key gaps in population and community ecology. *Front. Ecol. Environ.* 5 (3), 145–152.
- Albert, R., Jeong, H., Barabási, A.L., 1999. Internet: diameter of the world-wide web. *Nature* 401 (6749), 130–131.
- Alstott, J., Bullmore, E., Plenz, D., 2014. Powerlaw: a python package for analysis of heavy-tailed distributions. *PLoS One* 9, 1 e85777.
- Anderson, T., Dragićević, S., 2015. An agent-based modeling approach to represent infestation dynamics of the emerald ash borer beetle. *Ecol. Inform.* 30, 97–109.
- Anderson, T., Dragićević, S., 2016. Geospatial pest-parasitoid agent-based model for optimizing biological control of forest insect infestation. *Ecol. Modell.* 337, 310–329.
- Anderson, T., Dragicevic, S., 2018. Deconstructing geospatial agent-based model: sensitivity analysis of forest insect infestation model. In: Perez, L., Eun-Kyeong, K., Sengupta, R. (Eds.), *Agent Based Models and Complexity Science in the Age of Geospatial Big Data*. Springer, pp. 31–44.
- Andersson, E., Bodin, Ö., 2009. Practical tool for landscape planning? An empirical investigation of network based models of habitat fragmentation. *Ecography* 32 (1), 123–132.
- Andris, C., 2016. Integrating social network data into GI systems. *Int. J. Geogr. Inf. Sci.* 30 (10), 2009–2031.
- Anulewicz, A.C., McCullough, D.G., Cappaert, D.L., Poland, T.M., 2008. Host range of the emerald ash borer (*Agrilus planipennis* Fairmaire) (Coleoptera: Buprestidae) in North America: results of multiple-choice field experiments. *Environ. Entomol.* 37 (1), 230–241.
- Barabási, A.L., 2016. *Network Science*. Cambridge University Press, Cambridge, UK.
- Barabási, A.L., Albert, R., 1999. Emergence of scaling in random networks. *Science* 286 (5439), 509–512.
- Barthélemy, M., 2011. Spatial networks. *Phys. Rep.* 499 (1), 1–101.
- Berryman, M.J., Angus, S.D., 2010. Tutorials on agent-based modelling with NetLogo and network analysis with Pajek. *Complex Physical, Biophysical and Econophysical Systems*. pp. 351–375.
- BioForest Technologies Inc, 2011. TreeAzin Systemic Insecticide: Evidence for biennial Emerald Ash Borer treatments (*Agrilus planipennis* Fairmaire). Retrieved on December 21, 2017 from. Sault Ste. Marie: Bioforest Technologies Inc.. http://www.bioforest.ca/documents/assets/uploads/files/en/bioforest_2011_-_treeazin_2yr_efficacy.pdf
- Boccaletti, S., Latora, V., Moreno, Y., Chavez, M., Hwang, D., 2006. Complex networks: structure and dynamics. *Phys. Rep.* 424 (4–5), 175–308.
- Bone, C., Altaweel, M., 2014. Modeling micro-scale ecological processes and emergent patterns of mountain pine beetle epidemics. *Ecol. Modell.* 289, 45–58.
- Brown, D.G., Page, S., Riolo, R., Zellner, M., Rand, W., 2005. Path dependence and the validation of agent-based spatial models of land use. *Int. J. Geogr. Inf. Sci.* 19 (2), 153–174.
- Bunn, A.G., Urban, D.L., Keitt, T.H., 2000. Landscape connectivity: a conservation application of graph theory. *J. Environ. Manage.* 59 (4), 265–278.
- Cappaert, D., McCullough, D.G., Poland, T.M., Siegert, N.W., 2005. Emerald ash borer in North America: a research and regulatory challenge. *Am. Entomol.* 51 (3), 152–165.
- Cohen, J.E., 1978. *Food Webs and Niche Space*. Princeton University Press, New Jersey, NJ.
- Congalton, R.G., 1991. A review of assessing the accuracy of classifications of remotely sensed data. *Remote Sens. Environ.* 37 (1), 35–46.
- Dijkstra, E.W., 1959. A note on two problems in connection with graphs. *Numer. Math.* 1 (1), 269–271.
- Duan, J.J., Ulyshen, M.D., Bauer, L.S., Gould, J., Van Driesche, R., 2010. Measuring the impact of biotic factors on populations of immature emerald ash borers (Coleoptera: Buprestidae). *Environ. Entomol.* 39 (5), 1513–1522.
- Dupont, Y.L., Trojelsgaard, K., Olesen, J.M., 2011. Scaling down from species to individuals: a flower-visitation network between individual honeybees and thistle plants. *Oikos* 120 (2), 170–177.
- Erdos, P., Renyi, A., 1959. On random graphs. *Sel. Pap. Alfred Renyi* 2 (1), 308–315.
- Erdos, P., Renyi, A., 1960. On the evolution of random graphs. *Bull. Int. Stat. Inst.* 34 (4), 343–347.
- Ferrari, J.R., Lookingbill, T.R., Neel, M.C., 2007. Two measures of landscape-graph connectivity: assessment across gradients in area and configuration. *Landscape Ecol.* 22 (9), 1315–1323.
- Fortuna, M.A., Bascompte, J., 2007. The network approach in ecology. In: Valladares, F., Camacho, A., Elosegi, A., Gracia, C., Estrada, M., Senar, J.C., Gili, J.M. (Eds.), *Unity in Diversity: Ecological Reflections as a Tribute to Margalef*. Fundación BBVA, Bilbao, pp. 371–392.
- Fortuna, M.A., Gómez-Rodríguez, C., Bascompte, J., 2006. Spatial network structure and amphibian persistence in stochastic environments. *Proc. R. Soc. Lond. B Biol. Sci.* 273 (1592), 1429–1434.
- Grimm, V., Railsback, S.F., 2013. *Individual-Based Modeling and Ecology*. Princeton University Press, New Jersey, NJ.
- Grimm, V., Berger, U., Bastiansen, F., Eliassen, S., Ginot, V., Giske, J., Goss-Custard, J., Grand, T., Heinz, S.K., Huth, A., Jepsen, J.U., Jorgensen, C., Mooij, W.M., Buller, B., Pe'er, G., Piou, C., Railsback, S.F., Robbins, A.M., Rossmanith, E., Ruger, N., Strand, E., Souissi, S., Stillman, R.A., Vabo, R., Visser, U., DeAngelis, D.L., 2006. A standard protocol for describing individual-based and agent-based models. *Ecol. Modell.* 198 (1–2), 115–126.
- Guimera, R., Amaral, L.A.N., 2004. Modeling the world-wide airport network. *Eur. Phys. J. B Condens. Matter Complex Syst.* 38 (2), 381–385.
- Hall, S.J., Raffaelli, D.G., 1993. Food webs: theory and reality. *Adv. Ecol. Res.* 24, 187–239.
- Ings, T.C., Montoya, J.M., Bascompte, J., Blüthgen, N., Brown, L., Dormann, C.F., Lauridsen, R.B., 2009. Ecological networks—beyond food webs. *J. Anim. Ecol.* 78 (1), 253–269.
- Jennings, D.E., Taylor, P.B., Duan, J.J., 2014. The mating and oviposition behavior of the invasive emerald ash borer (*Agrilus planipennis*), with reference to the influence of host tree condition. *J. Pest Sci.* 87 (1), 71–78.
- Jiang, B., 2007. A topological pattern of urban street networks: universality and peculiarity. *Phys. A Stat. Mech. Appl.* 384 (2), 647–655.
- Jordano, P., 1987. Patterns of mutualistic interactions in pollination and seed dispersal: connectance, dependence asymmetries, and coevolution. *Am. Nat.* 129 (5), 657–677.
- Kirer, H., Çırpıcı, Y.A., 2016. A survey of agent-based approach of complex networks. *Ekonominik Yaklaşım* 27 (98), 1–28.
- Letcher, B.H., Rice, J.A., Crowder, L.B., Rose, K.A., 1996. Variability in survival of larval fish: disentangling components with a generalized agent-based model. *Can. J. Fish. Aquat. Sci.* 53 (4), 787–801.

- Lewis, T.G., 2011. Network Science: Theory and Applications. John Wiley & Sons, New Jersey, NJ.
- Lyons, D.B., Jones, G.C., 2005. The biology and phenology of the emerald ash borer. Proceedings, 16th US Department of Agriculture Interagency Research Forum on Gypsy Moth and Other Invasive Species. pp. 62–63.
- McCullough, D.G., Siegert, N.W., 2007. Estimating potential emerald ash borer (Coleoptera: Buprestidae) populations using ash inventory data. *J. Econ. Entomol.* 100 (5), 1577–1586.
- McCullough, D.G., Poland, T.M., Anulewicz, A.C., Cullough, D.G.M.C., 2009. Emerald ash borer (Coleoptera: Buprestidae) attraction to stressed or baited ash trees. *Environ. Entomol.* 38 (6), 1668–1679.
- Mercader, R.J., Siegert, N.W., Liebhold, A.M., McCullough, D.G., 2009. Dispersal of the emerald ash borer, *Agrilus planipennis*, in newly-colonized sites. *Agric. For. Entomol.* 11 (4), 421–424.
- Mercader, R.J., Siegert, N.W., Liebhold, A.M., McCullough, D.G., 2011. Influence of foraging behavior and host spatial distribution on the localized spread of the emerald ash borer, *Agrilus planipennis*. *Popul. Ecol.* 53 (2), 271–285.
- Minor, E.S., Urban, D.L., 2007. Graph theory as a proxy for spatially explicit population models in conservation planning. *Ecol. Appl.* 17 (6), 1771–1782.
- Morris, R.J., Lewis, O.T., Godfray, H.C.J., 2004. Experimental evidence for apparent competition in a tropical forest food web. *Nature* 428 (6980), 310–313.
- Muirhead, J.R., Leung, B., Overdijk, C., Kelly, D.W., Nandakumar, K., Marchant, K.R., MacIsaac, H.J., 2006. Modelling local and long-distance dispersal of invasive emerald ash borer *Agrilus planipennis* (Coleoptera) in North America. *Divers. Distrib.* 12 (1), 71–79.
- Muller, C.B., Adriaanse, I.C.T., Belshaw, R., Godfray, H.C.J., 1999. The structure of an aphid-parasitoid community. *J. Anim. Ecol.* 68 (2), 346–370.
- Newman, M.E., 2003. The structure and function of complex networks. *SIAM Rev.* 45 (2), 167–256.
- North, M.J., Collier, N.T., Ozik, J., Tatara, E.R., Macal, C.M., Bragin, M., Sydelko, P., 2013. Complex adaptive systems modeling with Repast Simphony. *Complex Adapt. Syst. Model.* 1 (1), 1–26.
- Parks Recreation and Culture Guide [Tabular Data], 2018. Oakville Open Data, July 10. Available: <https://portal-exploreoakville.opendata.arcgis.com/datasets/toak::parks-recreation-and-culture-guide>.
- Pascual-Hortal, L., Saura, S., 2008. Integrating landscape connectivity in broad-scale forest planning through a new graph-based habitat availability methodology: application to capercaillie (*Tetrao urogallus*) in Catalonia (NE Spain). *Eur. J. For. Res.* 127 (1), 23–31.
- Pereira, M., Segurado, P., Neves, N., 2011. Using spatial network structure in landscape management and planning: a case study with pond turtles. *Landsc. Urban Plan.* 100 (1), 67–76.
- Perez, L., Dragičević, S., 2010. Modeling mountain pine beetle infestation with an agent-based approach at two spatial scales. *Environ. Model. Softw.* 25 (2), 223–236.
- Rebek, E.J., Herms, D.a, Smitley, D.R., 2008. Interspecific variation in resistance to emerald ash borer (Coleoptera: Buprestidae) among North American and Asian ash (*Fraxinus* spp.). *Environ. Entomol.* 37 (1), 242–246.
- Repast Simphony, 2017. Version 2.4. [Computer Software]. University of Chicago, Chicago, IL.
- Road Network[Shapefile], 2018. Oakville Open Data, June 27. Available: and (Accessed July 16, 2018). https://portal-exploreoakville.opendata.arcgis.com/datasets/8b09936309264feeb57cb45f8018ab14_26.
- Rutledge, C.E., Keena, M.A., 2012. Mating frequency and fecundity in the emerald ash borer *Agrilus planipennis* (Coleoptera: Buprestidae). *Ann. Entomol. Soc. Am.* 105 (1), 66–72.
- Semeniuk, C.A.D., Musiani, M., Hebblewhite, M., Grindal, S., Marceau, D.J., 2012. Incorporating behavioral-ecological strategies in pattern-oriented modeling of caribou habitat use in a highly industrialized landscape. *Ecol. Model.* 243, 18–32.
- Siegert, N.W., McCullough, D.G., Liebhold, A.M., Telewski, F.W., 2014. Dendrochronological reconstruction of the epicentre and early spread of emerald ash borer in North America. *Divers. Distrib.* 20 (7), 847–858.
- Stang, M., Klinkhamer, P.G., Van Der Meijden, E., 2006. Size constraints and flower abundance determine the number of interactions in a plant-flower visitor web. *Oikos* 112 (1), 111–121.
- Stoneham, A.K.M., 1977. The small-world problem in a spatial context. *Environ. Plan A* 9 (2), 185–195.
- Stouffer, D.B., Fortuna, M.A., Bascompte, J., 2010. Ideas for moving beyond structure to dynamics of ecological networks. In: Boccaletti, S. (Ed.), *Handbook On Biological Networks*. World Scientific Publishing, Singapore, pp. 307–328.
- Straw, N.A., Williams, D.T., Kulinich, O., Gninenko, Y.I., 2013. Distribution, impact and rate of spread of emerald ash borer *Agrilus planipennis* (Coleoptera: Buprestidae) in the Moscow region of Russia. *Forestry* 86 (5), 515–522.
- Taylor, R.A., Poland, T.M., Bauer, L.S., Windell, K.N., Kautz, J.L., 2007. Emerald ash borer flight estimates revised. *Proceedings Of The Emerald Ash Borer/Asian Longhorned Beetle Research And Technology*. FHTET-2007-04.
- Thluczek, A.R., McCullough, D.G., Poland, T.M., 2011. Influence of host stress on emerald ash borer (Coleoptera: Buprestidae) adult density, development, and distribution in *Fraxinus pennsylvanica* trees. *Environ. Entomol.* 40 (2), 357–366.
- Travis, J.M., Dytham, C., 1998. The evolution of dispersal in a metapopulation: a spatially explicit, agent-based model. *Proc. R. Soc. Lond. B Biol. Sci.* 265 (1390), 17–23.
- Trees [Shapefile], 2018. Oakville Open Data, May 11. Available: and (accessed July 16, 2018). https://portalexploreoakville.opendata.arcgis.com/datasets/18bab686f6c4458b942c1c9830cf0d_0.
- Urban, D., Keitt, T., 2001. Landscape connectivity: a graph-theoretic perspective. *Ecology* 82 (5), 1205–1218.
- Watts, D.J., Strogatz, S.H., 1998. Collective dynamics of “small-world” networks. *Nature* 393 (6684), 440–442.
- Zetterberg, A., Mörberg, U.M., Balfors, B., 2010. Making graph theory operational for landscape ecological assessments, planning, and design. *Landsc. Urban Plan.* 95 (4), 181–191.